AIAA JOURNAL
Vol. 32, No. 8, August 1994

Linearized Theory for Pulse Tube Cryocooler Performance

Harold Mirels*
The Aerospace Corporation, El Segundo, California 90245

A linearized theory, which assumes small pressure perturbations, is presented for the performance of orifice-type pulse tube cryocoolers. The effect of gas-to-wall heat transfer within the pulse tube is included. Analytical expressions are derived for pulse tube flow properties and refrigeration power as functions of parameters K, H_1, and y, which characterize orifice area, pulse tube volume, and pulse tube thermal-layer thickness, respectively. The orifice area that optimizes refrigeration power is deduced. When operating with the optimum orifice area, the effect of the first-order (sinusoidal) gas-to-wall heat transfer, within the pulse tube, is to decrease refrigeration power. A basic (zero orifice area) pulse tube cryocooler is found to provide about 10% of the refrigeration power available from an orifice-type device. It is shown that a two-piston Stirling-cycle cryocooler provides greater refrigeration power than the corresponding conventional pulse tube cryocooler.

Nomenclature

A = cross-sectional area
a = function of y, Eqs. (12c) and (13a)
B = pressure perturbation parameter, Eq. (4b)
b = function of y, Eqs. (12c) and (13a)
G = Eq. (12i)
H_1 = pulse tube volume parameter, Eq. (14c)
K = orifice area parameter, Eqs. (12h) and (12j)
L_F = pulse tube length V_F/A_F
M = mass in compression, expansion, and dead space volumes
$\bar{P}$ = average power per cycle, Eq. (5)
$\bar{P}_E$ = normalized refrigeration power, Eq. (6)
p = pressure
p_m = mean pressure
Δp = pressure perturbation
R = gas constant, $p/\rho T$
r = characteristic semiwidth of pulse tube, Fig. 3
S = internal surface area of pulse tube
T = temperature
t = time
V = volume
X = piston displacement, Figs. 2 and 3
α = function of G and y, Eq. (12a)
$\bar{\alpha}$ = thermal diffusivity, $k/(\rho c_p)$
β = function of K, G, and y, Eq. (12b)
γ = ratio of specific heats, c_p/c_v
λ = characteristic (unbounded geometry) boundary-layer thickness, $\sqrt{2\bar{\alpha}/\omega}$
ρ = density
ϕ_e = phase of X_e relative to X_c, Eq. (1b)
ϕ_p = phase of Δp relative to X_c, Eq. (16a)
ω = frequency, rad/s

Subscripts

C, c = compression region
D = dead space
E, e = expansion region
F = gas spring region
g = exit region of pulse tube, Fig. 3

Received Dec. 16, 1992; revision received Sept. 20, 1993; accepted for publication Oct. 11, 1993.

*Principal Scientist, Mechanics and Materials Technology Center. Fellow AIAA.

Introduction

CRYCOOLERS[1,2] are refrigerators that generate temperatures in the range $T \leq 120$ K. Small-scale cryocoolers, with refrigeration powers in the order of a watt, are of interest for a variety of military and civilian applications. They are used for cooling infrared detectors in night vision, missile guidance, and satellite sensor systems. They are also of interest for devices employing high-temperature superconductors.

Refrigerators based on the Stirling cycle have emerged as leading candidates for these applications. The classical Stirling-cycle refrigerator has two crankshaft-driven pistons. These operate in the compression and expansion phases of the cycle, respectively. A modification of the classical configuration employs an expansion piston that is free floating. More recently, the free-floating piston has been replaced by a pulse tube. The analysis of the latter device is the subject of the present study.

A schematic representation of a pulse tube cryocooler is illustrated in Fig. 1. This system is referred to as an "orifice pulse tube refrigerator (OPTR)" in Ref. 3. The corresponding closed-end configuration (i.e., zero orifice area) is referred to as a "basic pulse tube refrigerator (BPTR)" in Ref. 3.

The first BPTR apparatus was described by Gifford and Longsworth[4,5] and Longsworth.[6] The origin of the refrigeration effect was attributed to "surface heat pumping"[5] wherein heat is transported from the cold end to the hot end of the pulse tube surface by the periodic motion of the working fluid. The concept of including an orifice and a reservoir was introduced by Mikulin et al.[7–9] This modification led to a significant increase in refrigerator performance. It is this device that is illustrated in Fig. 1. Further analytic and experimental study has been presented by Storch et al.[3] and Radebaugh and co-workers,[10–12] as well as by others.

A mathematical model for estimating OPTR performance is presented in Ref. 9. This model requires the numerical integration of a system of partial differential equations. Some numerical results were included in Ref. 9. A numerical model is also presented in Ref. 13. On the other hand, Ref. 3 provides analytic expressions for OPTR performance. However, the analytic model in Ref. 3 does not explicitly relate pulse tube performance to orifice area and does not consider the effect of heat transfer within the pulse tube. The theory of Ref. 3 does not apply to BPTR configurations.

The object of the present study is to develop an analytical model that includes the effect of heat transfer within the pulse tube and provides explicit expressions for BPTR/OPTR performance in terms of device geometry and operating temperature. It is assumed that the pressure, throughout the device, is uniform at each instant. A linearized theory is developed that is based on the assumption that piston-induced pressure perturbations are small. A gas spring hysteresis model, developed in Ref. 14, is used to model energy dissipation within the pulse tube. The study is a first-order analysis

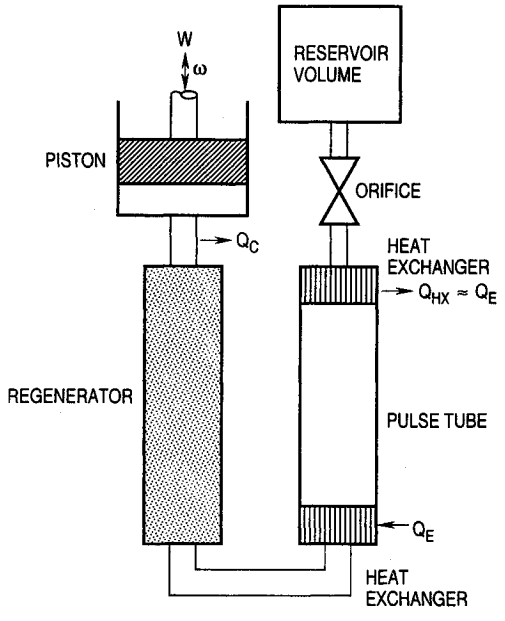

Fig. 1 Schematic representation of pulse tube cryocooler.

in the sense that parasitic losses[1] (e.g., thermal conduction, radiation, regenerator inefficiency) are neglected. The results of this study are expected to help define the important physical processes in the OPTR and to provide a basis for performance optimization.

Theory

A linearized version of the Stirling-cycle cryocooler analysis, due to Schmidt, is presented as described by Walker.[2] This is then generalized to describe pulse tube cryocooler performance.

Schmidt Theory

The geometry considered by Schmidt is illustrated in Fig. 2. Three volumes are considered; namely, a net compression volume, V_C, a net dead space volume, V_D (which is assumed not to vary with time and contains a regenerator), and a net expansion volume, V_E. Piston motion in the compression and expansion volumes results in time-dependent variations in V_C and V_E, which are denoted by lower-case subscripts; namely, V_c and V_e. It is assumed that the gas temperature in each of these volumes does not vary with time (i.e., isothermal compression and expansion in volumes V_C and V_E, respectively). These temperatures are denoted T_C, T_D, and T_E, respectively, where T_D represents the average temperature in volume V_D. The pressure is assumed uniform throughout the three volumes, at any instant, and varies with time. The assumption of isothermal processes in volumes V_C and V_E imply heat exchangers, which are indicated in Fig. 1, but have been omitted in Fig. 2. The assumption of an isothermal process in volume V_D implies a lossless regenerator.

Sinusoidal motion is assumed for each of the two pistons shown in Fig. 2. The piston displacements and corresponding volume variations can be expressed as

$$\frac{X_c}{X_C} = 1 - \frac{2V_c}{V_C} = \cos \omega t = e^{i\omega t} \tag{1a}$$

$$\frac{X_e}{X_E} = 1 - \frac{2V_e}{V_E} = \cos\,(\omega t + \phi_e) = e^{i(\omega t + \phi_e)} \tag{1b}$$

in accord with the definitions in Fig. 2. Use of the real parts of the complex expressions in Eq. (1) is implied. Let M denote the net mass of the working fluid in volumes V_C, V_D, and V_E. Using the equation of state, $p = \rho RT$, the pressure at each instant is

$$\frac{RM}{p} = \frac{V_c}{T_C} + \frac{V_D}{T_D} + \frac{V_e}{T_E} \tag{2}$$

The mean value of pressure is given by

$$\frac{RM}{p_m} = \frac{V_C}{2T_C} + \frac{V_D}{T_D} + \frac{V_E}{2T_E} \tag{3}$$

Subtraction of Eq. (3) from Eq. (2) yields a linearized expression for the pressure perturbation $\Delta p = p - p_m$, namely

$$\frac{1}{Be^{i\omega t}} \frac{\Delta p}{p_m} = \left(1 + \frac{V_E}{V_C} \frac{T_C}{T_E} e^{i\phi_e}\right)[1 + \mathcal{O}(B)] \tag{4a}$$

where B is the pressure perturbation parameter

$$B = p_m V_C / (2T_C RM) \ll 1 \tag{4b}$$

which is assumed to be small. Within the present approximation, B can be expressed

$$B = \frac{1}{2} \frac{V_C}{V_D} \frac{T_D}{T_C}[1 + 0(B)] \tag{4c}$$

which includes the relation $(V_E T_D)/(V_D T_E) = 0(B)$, in accord with Eq. (18a). Thus, B is approximately equal to the ratio of the average mass in the compression region divided by the mass in the dead space. The average power expended by the expansion piston is found from

$$\frac{P_E}{A_E} = \frac{\omega}{2\pi} \int_0^{2\pi/\omega} \Delta p(-\dot{X}_e)\, dt = \frac{1}{2} R.P.\,[\Delta p(-\dot{X}_e)^*] \tag{5}$$

where $R.P.$ and $(\,)^*$ denote real part and complex conjugate, respectively, and A_E is the cross-sectional area. In accord with a Stirling thermodynamic-cycle analysis, the expansion piston power P_E equals the power expended by the gas in volume V_E during its isothermal expansion, and thus equals refrigeration power. Normalized expressions for refrigeration power P_E and the corresponding compression piston power P_C are

$$\bar{P}_E \equiv \frac{8(T_C/T_E)P_E}{\omega B p_m V_C} = 2 \frac{V_E}{V_C} \frac{T_C}{T_E} \sin \phi_e \tag{6}$$

$$\bar{P}_C \equiv \frac{8(T_C/T_E)P_C}{\omega B p_m V_C} = \frac{T_C}{T_E} \bar{P}_E \tag{7}$$

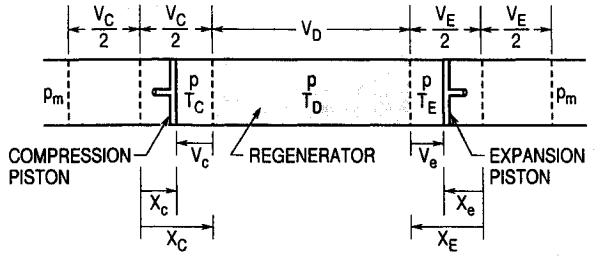

Fig. 2 Notation for Schmidt model of a classical Stirling-cycle cryocooler.

The coefficient of performance (COP) of the cryocooler equals the refrigeration power P_E divided by the net input power. For cases where the expansion piston drives a crankshaft,

$$\text{COP} = \frac{P_E}{P_C - P_E} = \frac{T_E}{T_C - T_E} \tag{8}$$

which corresponds to a Carnot efficiency. For cases where the expansion piston does no useful work (e.g., free piston cryocooler), the coefficient of performance is

$$\text{COP} = \frac{P_E}{P_C} = \frac{T_E}{T_C} \tag{9}$$

The latter expression is applicable to pulse tube cryocoolers.

Pulse Tube Cyrocooler

The pulse tube cryocooler can be considered a variant of a Stirling-cycle cryocooler wherein the expansion piston is replaced by a gas spring that contains an orifice. The correspondence is illustrated in Fig. 3. The piston in Fig. 3 is, in fact, a contact surface between the expansion gas (volume V_E) and the gas spring (volume V_F). The boundary condition across the contact surface requires that the particle velocity and pressure be continuous. The displacement and phase of the contact surface is initially unknown and is evaluated in the present section. We assume

$$V_E/V_F \ll 1 \tag{10}$$

which is consistent with $\Delta p/p_m \ll 1$. Thus, V_F is essentially equal to the net pulse tube volume and is considered a known quantity (Fig. 3).

The performance of a gas spring with both gas-to-wall thermal conduction and orifice flow has been investigated in Ref. 14. From Ref. 14, the relation between X_e and Δp is

$$(-1)\,\gamma\frac{X_e}{L_F} = (\alpha - i\beta)\,(\Delta p/p_m) \tag{11}$$

where $L_F = V_F/A_F$. The parameters α and β equal

$$\alpha = 1 + Gb \tag{12a}$$

$$\beta = K + Ga \tag{12b}$$

where

$$a + ib = \frac{(\sinh 2y - \sin 2y) + i\,(\sinh 2y + \sin 2y)}{y\,(\cosh 2y + \cos 2y)} \tag{12c}$$

$$= [\,(4/3)\,y^2 + 2i\,]\,[1 + \mathcal{O}(y^4)] \qquad y \ll 1 \tag{12d}$$

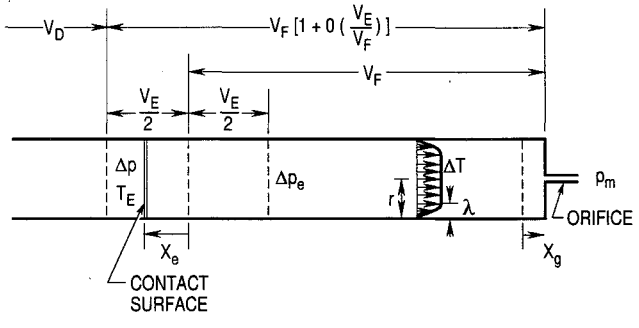

Fig. 3 Notation for pulse tube portion of a pulse tube cryocooler; contact surface is equivalent to expansion piston in Fig. 2.

$$= \left[\frac{1}{y} + \frac{i}{y}\right][1 + \mathcal{O}(e^{-2y})] \qquad y \gg 1 \tag{12e}$$

$$y = r/\lambda \tag{12f}$$

$$\lambda = (2\bar{\alpha}/\omega)^{1/2} \tag{12g}$$

$$K = \frac{\gamma}{\omega}\frac{\dot{X}_g/L_F}{(\Delta p)/p_m} \tag{12h}$$

$$G = [\,(\gamma - 1)/2]\,(Sr/V_F) \tag{12i}$$

The quantities a and b define the net gas-to-wall heat transfer rate $(-\Delta\dot{Q})$ in the pulse tube (i.e., $a + ib \sim (-\Delta\dot{Q})/\Delta p$). These are functions of the parameter $y = r/\lambda$, where r is the pulse tube semiwidth and λ is the thermal boundary-layer thickness corresponding to infinite wall separation. To first order, the heat transfer has a sinusoidal variation, and there is no net transfer of heat to the wall. The amplitude of the first-order sinusoidal heat transfer increases monatomically as y decreases from ∞ (isentropic limit) to 0 (isothermal limit). A second-order solution does provide a net transfer of heat, from gas to wall, per cycle. The latter is zero in the limits $y = 0$ and ∞ and is a maximum at $y = \mathcal{O}(1)$ (Ref. 14). The parameter K is proportional to the volume change due to orifice flow divided by the volume change due to the gas spring piston displacement. Hence, K is a measure of the relative importance of the orifice flow. For Poiseuille flow through the orifice

$$\mathrm{K} = \gamma\pi p_m R^4/(8\mu L\omega V_F) \tag{12j}$$

where μ, R, and L are viscosity, orifice radius, and orifice length, respectively.

The coefficient Sr/V_F in Eq. (12i) defines the pulse tube surface-to-volume ratio. Equations (12c–12e) have been derived[14] for a pulse tube bounded by two parallel walls ($Sr/V_F = 1$). Corresponding expressions for a cylindrical pulse tube ($Sr/V_F = 2$) are[14]

$$a + ib = \frac{-\sqrt{-2i}}{y}\frac{J_1(y\sqrt{-2i})}{J_0(y\sqrt{-2i})} \tag{13a}$$

$$= \left(\frac{y^2}{4} + i\right)[1 + \mathcal{O}(y^4)] \qquad y \ll 1 \tag{13b}$$

$$= \left(\frac{1}{y} + \frac{i}{y}\right)[1 + \mathcal{O}(e^{-2y})] \qquad y \gg 1 \tag{13c}$$

where J_n denotes the Bessel function of order n. Equations (12c) and (13a) agree in the limit $y \gg 1$. In this limit, Eq. (12c) is applicable for arbitrary geometry, provided the appropriate value of Sr/V_F is used.

Equations (1b) and (4a) are substituted into Eq. (11). Equating real and imaginary parts yields

$$\frac{T_C}{T_E}\frac{V_E}{V_C} = \frac{[\,(\alpha H_1)^2 + (\beta H_1)^2\,]^{1/2}}{[\,(1 + \alpha H_1)^2 + (\beta H_1)^2\,]^{1/2}} \tag{14a}$$

$$\left.\begin{aligned}\sin\phi_e &= \beta H_1/[\,(\alpha H_1)^2 + (\beta H_1)^2\,]^{1/2}\\ \pi/2 &\le \phi_e \le \pi\end{aligned}\right\} \tag{14b}$$

where

$$H_1 = \frac{1}{\gamma}\frac{V_F}{T_E}\frac{p_m}{RM} = \frac{2B}{\gamma}\frac{T_C}{T_E}\frac{V_F}{V_C} \tag{14c}$$

is a measure of pulse tube volume. Equations (14a) and (14b) define, respectively, the amplitude and the phase of the contact surface motion. The phase angle ϕ_e, is in the second quadrant. The ratio V_E/V_F is found from Eq. (14a) using

$$\frac{\gamma H_1}{2B}\frac{V_E}{V_F} = \frac{V_E}{V_C}\frac{T_C}{T_E} \tag{15}$$

The pressure perturbation is uniform throughout the device and equals

$$\frac{1}{B}\frac{\Delta p}{p_m} = \frac{e^{i(\omega t+\phi_p)}}{(1+\alpha H_1)^2+(\beta H_1)^2} \tag{16a}$$

where

$$\tan\phi_p = \frac{\beta H_1}{1+\alpha H_1} \tag{16b}$$

The average power expended by the contact surface is denoted P_E and can be obtained from Eqs. (6), (14a), and (14b). The result, in normalized form, is

$$\bar{P}_E \equiv \frac{8(T_C/T_E)P_E}{\omega B p_m V_C} = \frac{2\beta H_1}{(1+\alpha H_1)^2+(\beta H_1)^2} \tag{17}$$

which defines refrigeration power. Equations (14–17) express cryocooler performance in terms of the two variables αH_1 and βH_1. The variation of $\bar{P}_E$, $(T_C V_E)/(T_E V_C)$, and $\sin\phi_e$ with βH_1, for fixed values of αH_1, is given in Figs. 4a–4c, respectively. These results are discussed later. Upper bounds on expansion volume and refrigeration power are

$$\frac{T_C}{T_E}\frac{V_E}{V_C} \le 1 \tag{18a}$$

$$\bar{P}_E \le 1 \tag{18b}$$

Equations (10) and (15) indicate the requirement

$$H_1 \gg \frac{2B}{\gamma}\left(\frac{T_C}{T_E}\frac{V_E}{V_C}\right) \tag{19}$$

for model consistency.

Optimization

The optimization of refrigeration power is now considered. The variation of $\bar{P}_E$ with βH_1, for fixed αH_1, has a local maximum (Fig. 4). The maximum occurs at [from Eq. (17)]

$$\beta H_1 = 1+\alpha H_1 \tag{20a}$$

and has the value

$$\bar{P}_E = 1/(1+\alpha H_1) \tag{20b}$$

Other quantities of interest at this maximum are

$$\frac{T_C}{T_E}\frac{V_E}{V_C} = \frac{1}{2^{1/2}}\left[1+\left(\frac{\alpha H_1}{1+\alpha H_1}\right)^2\right]^{1/2} \tag{21a}$$

$$\sin\phi_e = [1+(1+2\alpha H_1)^2]^{-1/2} \tag{21b}$$

$$\left|\frac{1}{B}\frac{\Delta p}{p_m}\right| = [2^{1/2}(1+\alpha H_1)]^{-1} \tag{21c}$$

$$\phi_p = \pi/4 \tag{21d}$$

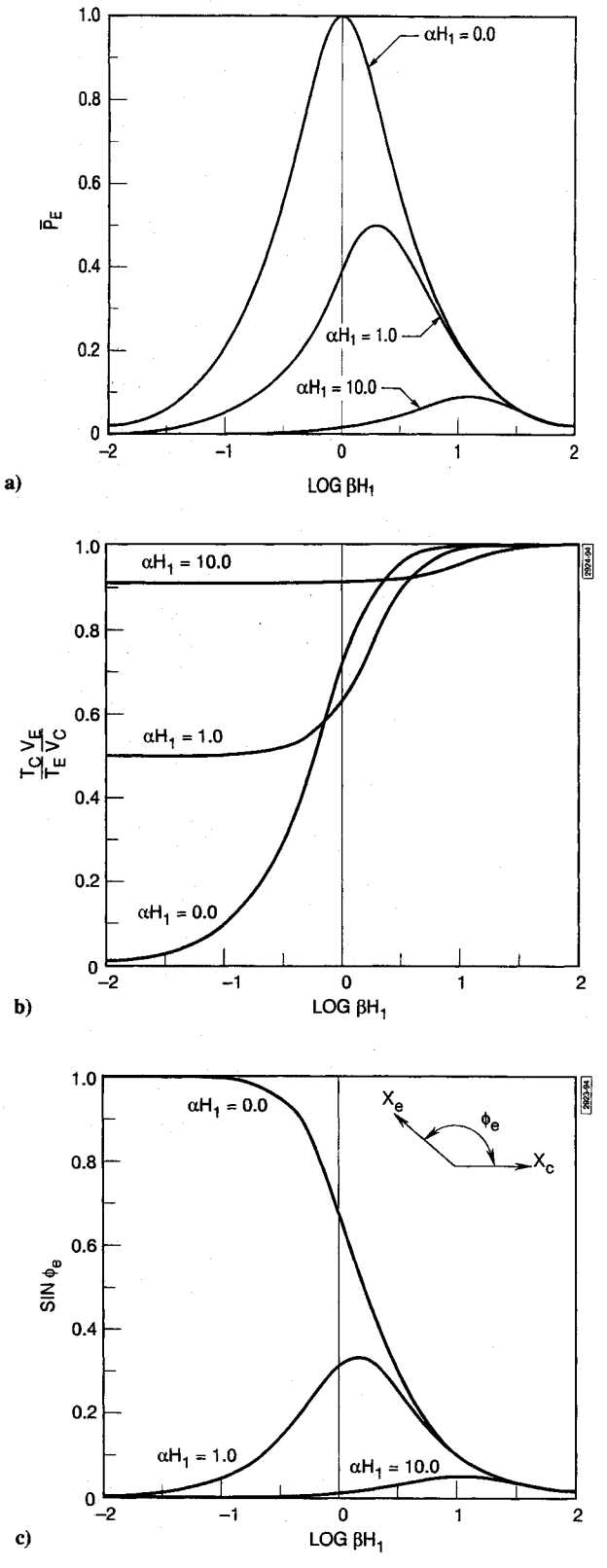

Fig. 4 Variation of pulse tube performance with βH_1 for αH_1 = 0.0, 1.0, and 10.0: a) $\bar{P}_E$, b) $(T_C/T_E)(V_E/V_C)$, and c) sin ϕ_e.

Equation (20b) indicates that $\bar{P}_E \to 1$ as $\alpha H_1 \to 0$. The present linearized model, however, requires $H_1 \gg 2^{1/2}B/\gamma$ [Eqs. (19) and (21a)]. The increase in $\bar{P}_E$ with decrease in αH_1 is due to the inverse relation between Δp and αH_1 [Eq. (21c)] and is expected to be observed in a nonlinear model. In a practical device, the limitation on how small H_1 can be made is probably associated with the requirement that the cold gas in the expansion region not communicate with the high-temperature heat exhanger near the orifice.

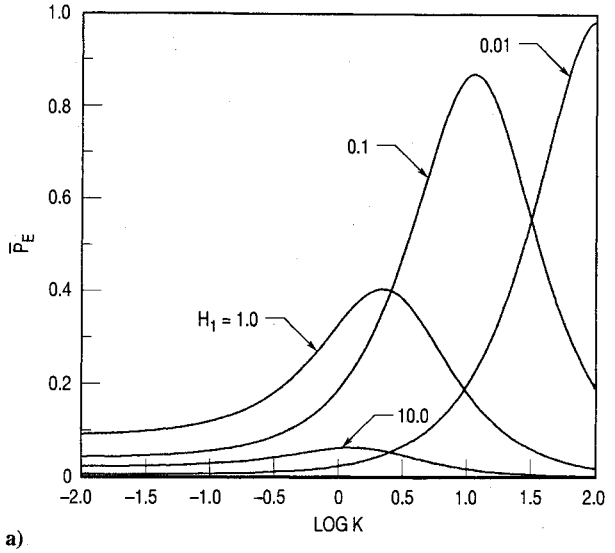

a)

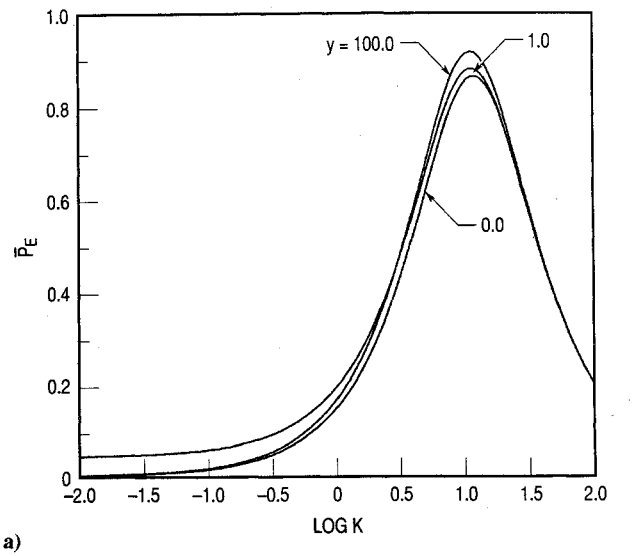

a)

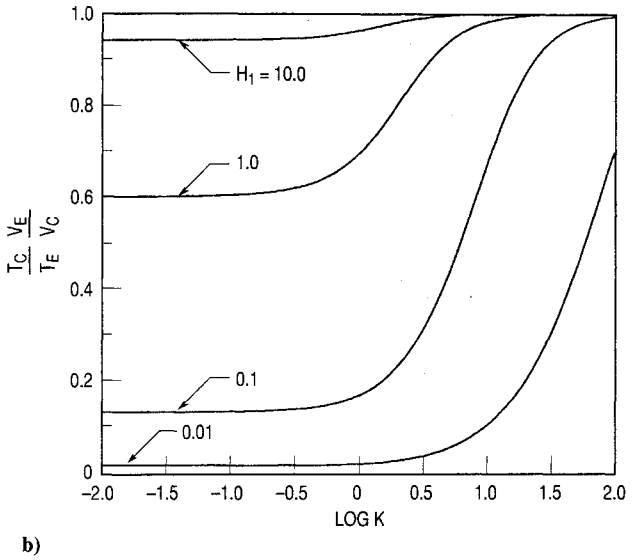

b)

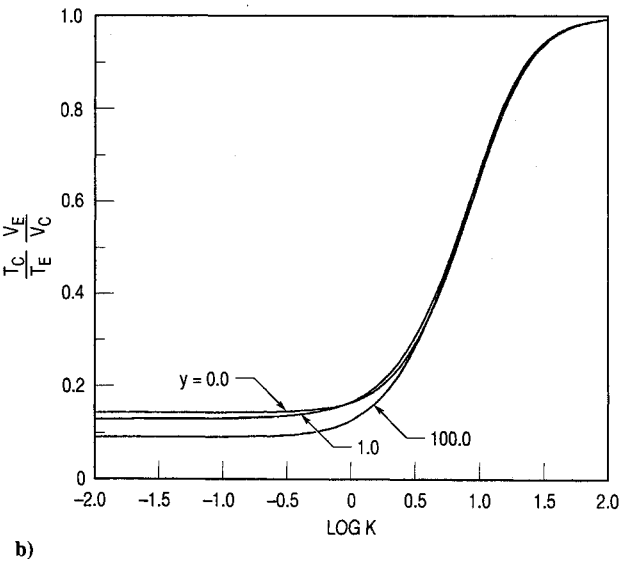

b)

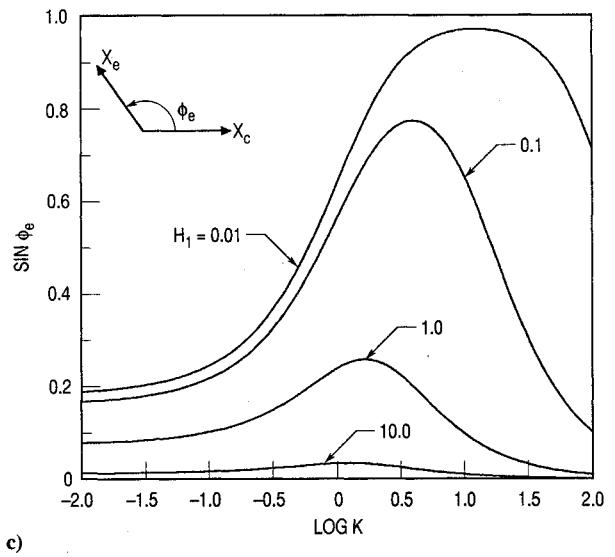

c)

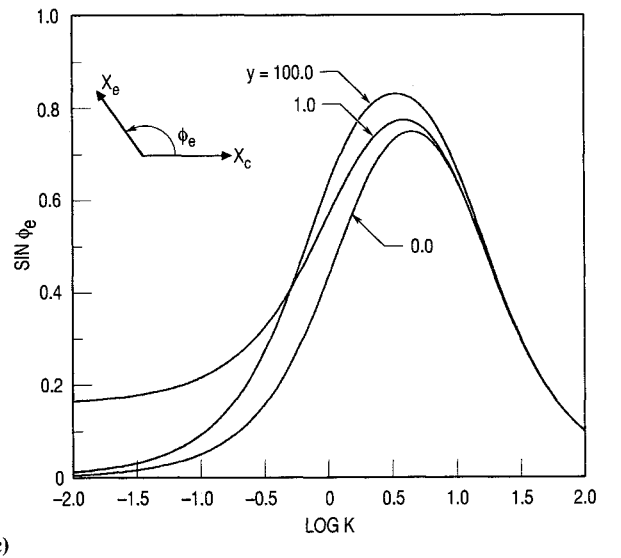

c)

Fig. 5 Variation of pulse tube performance with K for cases G = 1/3, y = 1.0, and H_1 = 0.01, 0.1, 1.0, and 10.0: a) $\bar{P}_E$, b) $(T_C/T_E)(V_E/V_C)$, and c) sin ϕ_e.

Fig. 6 Variation of pulse tube performance with K for cases G = 1/3, H_1 = 0.1, and y = 0.0, 0.1, 1.0, 10.0, and 100.0: a) $\bar{P}_E$, b) $(T_C/T_E)(V_E/V_C)$, and c) sin ϕ_e.

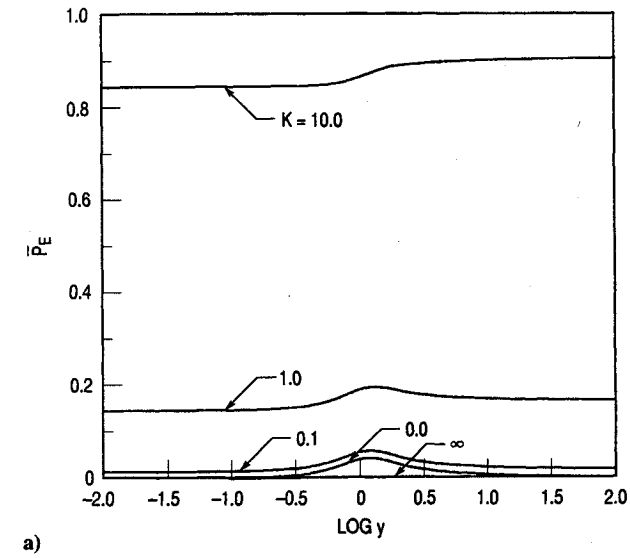

a)

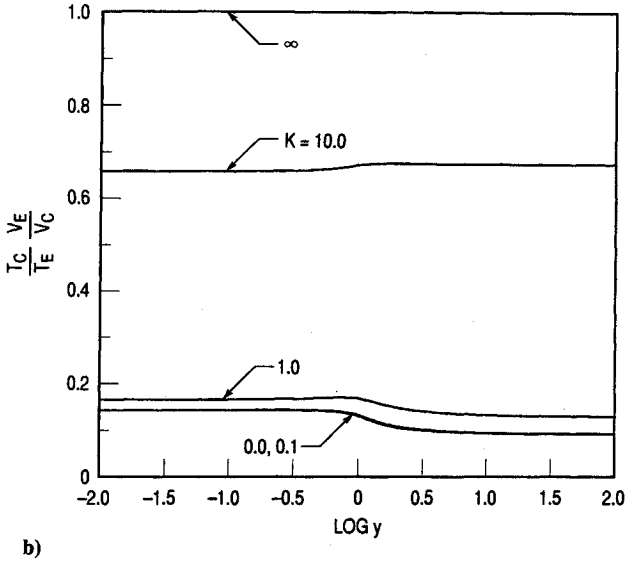

b)

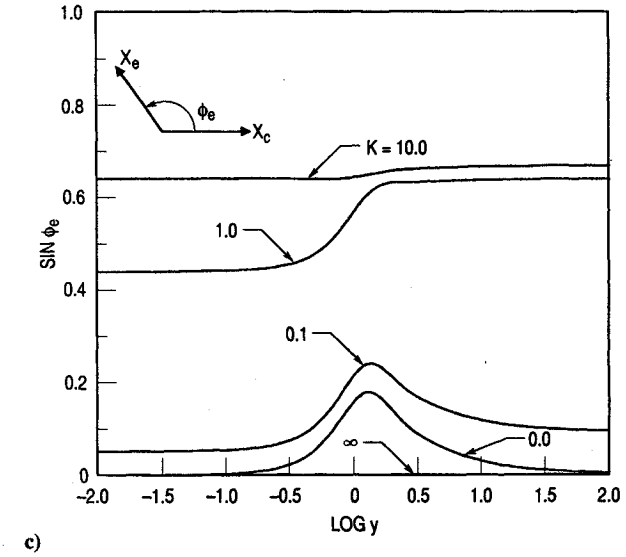

c)

Fig. 7 Variation of pulse tube performance with y for cases G = 1/3, H_1 = 0.1, and K = 0.0, 0.1, 1.0, 10.0, and ∞: a) $\bar{P}_E$, b) $(T_C/T_E)(V_E/V_C)$, and c) sin ϕ_e.

For a given value of H_1 and y, the optimum value of the orifice flow parameter K is, from Eq. (20a),

$$K = [(1 + \alpha H_1)/H_1] - Ga \tag{22}$$

It is seen that $K \to \infty$ as $H_1 \to 0$, which puts a further limit on how small H_1 can be made. For $y \to 0$, the optimum values of K and $\bar{P}_E$ are

$$K_0 = (1 + \gamma H_1)/H_1 \tag{23a}$$

$$\bar{P}_{E,0} = 1/(1 + \gamma H_1) \tag{23b}$$

and for $y \to \infty$

$$K_\infty = (1 + H_1)/H_1 \tag{24a}$$

$$\bar{P}_{E,\infty} = 1/(1 + H_1) \tag{24b}$$

Also,

$$K_0 K_\infty = (1 + \gamma H_1)/(1 + H_1) \geq 1 \tag{25a}$$

$$\bar{P}_{E,0}\,\bar{P}_{E,\infty} = (1 + H_1)/(1 + \gamma H_1) \geq 1 \tag{25b}$$

Equations (25) indicate that $K_0/K_\infty \geq 1$ and $\bar{P}_{E,0}/\bar{P}_{E,\infty} \leq 1$. Thus, the effect of the first-order periodic gas-to-wall heat transfer is to increase the optimum K and to decrease the maximum value of $\bar{P}_E$. The effect is small when H_1 is small and increases as H_1 increases. The decrease in refrigeration power with increase in heat transfer has been observed experimentally.[11]

The value of H_1, which yields maximum power, for the case of fixed α and β (i.e., fixed K and y) is

$$H_1 = (\alpha^2 + \beta^2)^{-1/2} \tag{26a}$$

and the corresponding power is

$$\bar{P}_E = \frac{\beta}{\alpha + (\alpha^2 + \beta^2)^{1/2}} \tag{26b}$$

Equations (26) are useful for optimizing the performance of a basic (K = 0) pulse tube, as will be discussed.

Numerical Results and Discussion

Numerical results have been obtained for the variation of pulse tube cryocooler performance with K, y, and H_1. These results are presented in Figs. 5–8. The value G = 1/3 (i.e., γ = 5/3, Sr/V_F = 1.0) is assumed.

The variation of $\bar{P}_E$ with K for y = 1 and $0.01 \leq H_1 \leq 10.0$ is given in Fig. 5a. As previously noted, these curves indicate that for a fixed pulse tube geometry (i.e., fixed H_1) and fixed y, there is an optimum value of orifice area for obtaining maximum refrigeration power. This result is in accord with the experiment. The values of $\bar{P}_E$ and K, at the maximum point, are given by Eqs. (20b) and (22). Corresponding values of the expansion volume and the expansion phase are given in Figs. 5b and 5c, respectively.

The variation of P_E with K, for H_1 = 0.1 and $0.0 \leq y \leq 100.0$, is indicated in Fig. 6a. A relatively small value of H_1 was chosen so that the maximum value of $\bar{P}_E$ is near 1.0. At the maximum power point, $K \approx 10$, the refrigeration power decreases by about 6% as y decreases from 100 (near isentropic flow) to 0 (isothermal flow). This result is in accord with Eq. (25b). The variation of expansion-volume parameters is given in Figs. 6b and 6c. Due to the small value of H_1, the parameters in Fig. 6 are relatively insensitive to y for $K \geq 0(1)$. For smaller values of K, energy dissipation within the orifice plays a lesser role, and cryocooler performance becomes dependent on the net second-order heat transfer from gas to wall.

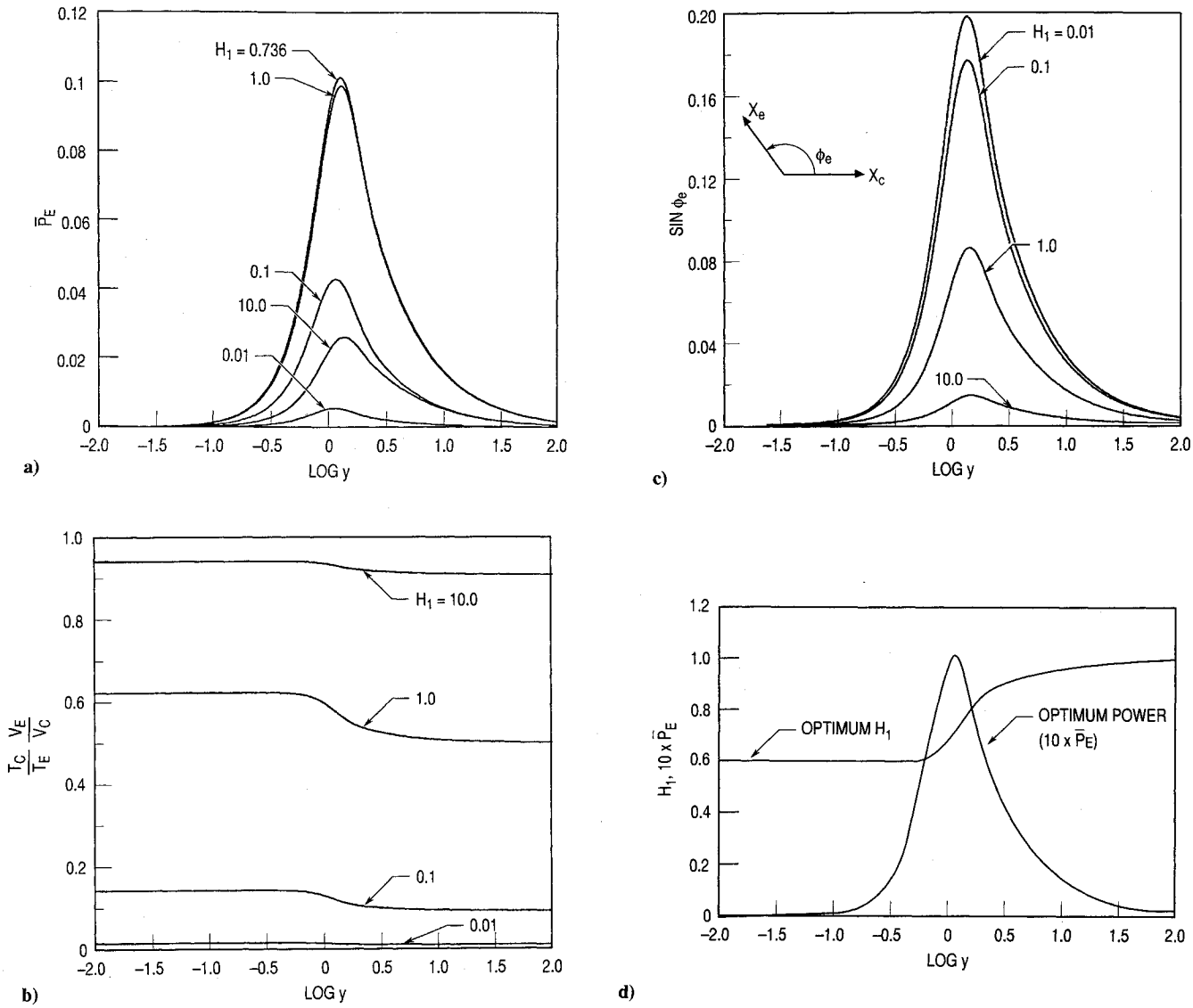

Fig. 8 Variation of pulse tube performance with y for cases $G = 1/3$, $K = 0$, and values of H_1 in the range $0.01 \le H_1 \le 10.0$: a) $\bar{P}_E$, b) $(T_C/T_E)(V_E/V_C)$, c) sin ϕ_e, and d) optimum H_1 and corresponding $\bar{P}_E$.

In the limit K→ 0, there is an optimum value of y (which maximizes the net heat transfer), as will be seen from Fig. 8.

Figures 7a–7c provide the variation of pulse tube parameters with y for $H_1 = 0.1$ and $0.0 \le K \le \infty$. The insensitivity of the parameters to y, for $K \ge 0(1)$, is again noted and is a consequence of $H_1 = 0.1$.

Figures 8a–8d provide results for a basic pulse tube ($K = 0$). The variation of $\bar{P}_E$ with y, for $0.01 \le H_1 \le 10.0$ is given in Fig. 8a. The power is a maximum; $\bar{P}_E = 0.101$, for $H_1 = 0.736$, and $y = 1.253$ [see Eq. (26)]. For other values of y, the optimum value of H_1 and the corresponding value of $\bar{P}_E$ is given by Fig. 8d and Eq. (26). The optimum power $\bar{P}_E$ decreases rapidly with departure of y from $y = 1.253$. The latter is the value of y for which the net (second-order) heat transfer from gas to wall is a maximum. The preceding results apply for $\gamma = 5/3$. When $\gamma = 7/5$, the power is a maximum; $\bar{P}_E = 0.068$, for $H_1 = 0.819$ and $y = 1.210$. Thus, for $\gamma = 5/3$ and $\gamma = 7/5$, the basic pulse tube provides about 10% and 7%, respectively, of the refrigeration power available from an orifice-type pulse tube.

Concluding Remarks

A linearized theory has been presented for orifice-type pulse tube cryocooler performance. Small pressure perturbations have been assumed. The effect of gas-to-wall heat transfer, within the pulse tube, has been included. Closed-form expressions have been found for normalized refrigeration power $\bar{P}_E$, as well as other flow properties, as a function of the two variables αH_1 and βH_1. These variables depend, in turn, on K, y, and H_1.

The pulse tube portion of the cryocooler has been represented by a gas spring with an orifice. Refrigeration power $\bar{P}_E$ equals the power expended by the contact surface that separates the expansion region from the gas spring. The contact surface plays the role of the expansion piston in a conventional Stirling cryocooler. The power expended by the contact surface (refrigeration power) equals the power dissipated within the orifice plus the net heat transfer from the gas to the wall within the pulse tube. For a given configuration, there is an orifice area that maximizes refrigeration power. When operating with an optimum orifice area, the effect of the first-order periodic heat transfer to the wall, as characterized by y, is detrimental to refrigeration power. The latter result is in accord with experiment[11] and suggests that surface heat pumping invoked by previous authors[5,15] is not a major contributor to orifice-type pulse tube refrigeration power. However, the effect of convection on the heat transfer within a pulse tube has not been considered in the present study. Inclusion of convection effects may indicate a more significant role for the effect of heat transfer on orifice pulse tube refrigeration power.

The configuration in Fig. 1 may be termed a conventional pulse tube cryocooler. The normalization of $\bar{P}_E$ is such that conventional pulse tube cryocooler power is limited to values in the range

$\bar{P}_E \leq 1$. In the absence of an orifice, $\bar{P}_E$ is limited to values in the range $\bar{P}_E \lesssim 0.1$. Hence, the presence of an orifice greatly increases refrigeration power. The value of $\bar{P}_E$ for a conventional two-piston Stirling-cycle cryocooler is [from Eq. (6)]

$$(\bar{P}_E)_{SC} = 2\left(\frac{V_E}{V_C}\frac{T_C}{T_E}\right)\sin\phi_e \tag{27}$$

Here, ϕ_e and $(V_E/V_C)(T_C/T_E)$ are design variables. By choosing $\phi_e = \pi/2$ and $(V_E/V_C)(T_C/T_E) \equiv N > 1$, the Stirling-cycle cryocooler provides $2N$ times the refrigeration obtained from a corresponding pulse tube cryocooler. Hence, the two-piston Stirling-cycle cryocooler provides more refrigeration than the corresponding pulse tube cryocooler. The coefficient of performance equals $T_E/(T_C - T_E)$ and T_E/T_C, respectively, for these devices. The use of a stepped piston and a bypass permits pulse cryocoolers to achieve $\bar{P}_E > 1$, but at the expense of thermal effiiciency.[16,17]

Acknowledgment

The present study was supported by the Aerospace Sponsored Research program.

References

[1]Walker, G., *Miniature Refrigerators for Cryogenic Sensors and Cold Electronics*, Clarendon Press, Oxford, England, UK, 1989, pp. 1–11, 105.

[2]Walker, G., *Cryocoolers Part 1: Fundamentals*, Plenum Press, New York, 1983, pp. 1–28, 134–142.

[3]Storch, P. J., Radebaugh, R., and Zimmerman, J. E., "Analytical Model for the Refrigeration Power of the Orifice Pulse Tube Refrigerator," National Inst. of Science and Technology TN 1343, 1990.

[4]Gifford, W. E., and Longsworth, R. C., "Pulse-Tube Refrigeration," *Transactions of the ASME*, Vol. 63, 1964, p. 264.

[5]Gifford, W. E., and Longsworth, R. C., "Surface Heat Pumping," *Advances in Cryogenic Engineering*, Vol. 11, Plenum Press, New York, 1966, p. 171.

[6]Longsworth, R. C., "An Experimental Investigation of Pulse Tube Refrigeration Heat Pumping Rates," *Advances in Cryogenic Engineering*, Vol. 12, Plenum Press, New York, 1967, p. 608.

[7]Mikulin, E. I., Shkrebyonock, M. P., and Tarasov, A. A., "Investigation of Cryogenic Pulse Tube," *Higher Educational Institutions News, Machinery Engineering*, Vol. 1, 1983, p. 71 (in Russian).

[8]Mikulin, E. I., Shkrebyonock, M. P., and Tarasov, A. A., "Expansion Cryogenic Pulse Tube," *Higher Educational Institutions News, Machinery Engineering*, Vol. 9, 1982, p. 76 (in Russian).

[9]Mikulin, E. I., Tarasov, A. A., and Schkrebyonock, M. P., "Low Temperature Expansion Pulse Tubes," *Advances in Cryogenic Engineering*, Vol. 29, Plenum Press, New York, 1984, p. 629.

[10]Radebaugh, R., Zimmerman, J., Smith, D. R., and Louie, B., "A Comparison of Three Types of Pulse Tube Refrigerators: New Methods for Reaching 60 K," *Advances in Cryogenic Engineering*, Vol. 31, Plenum Press, New York, 1986, p. 1979.

[11]Radebaugh, R., and Herrmann, S., "Refrigeration Efficiency of Pulse Tube Refrigerators," *Proceedings of the 4th International Cryocooler Conference*, David Taylor Naval Ship Research and Development Center, Bethesda, MD, 1987, p. 119.

[12]Radebaugh, R., Chowdhury, K., and Zimmerman, J., "Optimization of a Pulse Tube Refrigerator for a Fixed Compressor Swept Volume," *Proceedings of the 5th International Cryocooler Conference*, Naval Postgraduate School, Monterey, CA, 1988, p. 133.

[13]Wang, C., Wu P., and Chen, Z., "Numerical Modelling of an Orifice Pulse Tube," *Cryogenics*, Vol. 32, No. 9, 1992, pp. 785–790.

[14]Mirels, H., "Effect of Orifice Flow and Heat Transfer on Gas Spring Hysteresis," *AIAA Journal*, Vol. 32, No. 8, pp. 1656–1661.

[15]Lee, J. M., and Dill, H. R., "The Influence of Gas Velocity on Surface Heat Pumping for the Orifice Pulse Tube Refrigerator," *Cryogenic Engineering Conference* (Los Angeles), July 1989.

[16]Zhou, B., Wu, P., and Hu, S., "Experimental Results of the Internal Process of a Double Inlet Pulse Tube Refrigerator," *Cryogenics*, Vol. 32, Intersociety Energy Conversion Engineering Conference Supplement, 1992, pp. 24–27.

[17]Mirels, H., "Double Inlet Pulse Tube Cryocooler Theory," *Advances in Cryogenic Engineering*, Vol. 39, Plenum Press, New York, 1994.